Structural Instability of Shell-Like Assemblies of a Keplerate-Type Polyoxometalate Induced by Ionic Strength

ARTICLE *in* THE JOURNAL OF PHYSICAL CHEMISTRY B · NOVEMBER 2009

Impact Factor: 3.3 · DOI: 10.1021/jp907631a · Source: PubMed

2 AUTHORS:

Sandra Joyce Veen
Unilever
11 PUBLICATIONS **221** CITATIONS
SEE PROFILE

Willem K Kegel
Utrecht University
72 PUBLICATIONS **1,688** CITATIONS
SEE PROFILE

ARTICLES

Structural Instability of Shell-Like Assemblies of a Keplerate-Type Polyoxometalate Induced by Ionic Strength

Sandra J. Veen and Willem K. Kegel*

Van 't Hoff Laboratory for Physical and Colloid Chemistry, Debye Institute, Utrecht University, Padualaan 8, 3584 CH Utrecht, The Netherlands

Received: August 7, 2009; Revised Manuscript Received: September 18, 2009

We demonstrate a new structural instability of shell-like assemblies of polyoxometalates. Besides the colloidal instability, that is, the formation of aggregates that consist of many single layered POM-shells, these systems also display an instability on a structural scale within the shell-like assemblies. This instability occurs at significantly lower ionic strength than the colloidal stability limit and only becomes evident after a relatively long time. For the polyoxometalate, abbreviated as $\{Mo_{72}Fe_{30}\}$, it is shown that the structural stability limit of POM-shells lies between a NaCl concentration of 1.00 and 5.00 mM in aqueous solution.

Spontaneously assembling systems are of interest in both applied as well as fundamental sciences. They are widely used for the development of complex, functional structures. Each assembled system also has its limits within which it remains in its assembled state. The limits beyond which these systems are no longer stable as well as the nature of the instability give more insight in the forces governing the assembly and are therefore just as important as the process that drives the building blocks together.

One type of system that has been shown to spontaneously assemble into large superstructures are solutions of polyoxometalates (POMs). POMs are large, highly symmetrical inorganic molecules, consisting of (mainly) metal oxide polyhedrals (molybdenum, tungsten, vanadium, iron, etc). In solution they spontaneously form hollow, spherical assemblies with an average radius in water of several tens of nanometers and composed of a monolayer of more than 1000 of individual POM macro ions[1,2] (Figure 1). The formation of these intriguing shell-like assemblies or POM-shells is observed for POMs containing tungsten as well as POMs containing molybdenum or copper.[3] Besides the spherically shaped Keplerate-type POMs, wheel-shaped POMs have been shown to form these type of shell-like assemblies.[1,2] Moreover, even quite different systems, that is, metal-organic nanocages containing palladium,[4] form shell-like structures whose properties are well-described by the charge regulation model put forward in ref 5.

Once these POM-shells have been formed they display classical colloidal behavior in solution. The charged POM-shells can for instance be destabilized by increasing the ionic strength. As a result, the coulomb interactions between the POM-shells are screened upon which they aggregate and subsequently precipitate out of solution.[6] The concentration at which this aggregation is observed is dependent on the valency of the counterions, as is described by the classical Schultz-Hardy rule,[7] see ref 8. Here we demonstrate another instability in POM-shells: an instability based on a structural change in the POM-shells themselves. We here present evidence as well as a theoretical explanation of the new experimental stability limit for a system of POM-shells.

In previous research it has been shown that, given their existence, the behavior of the POM-shells can be very well described by a stabilization mechanism based on charge regulation.[5] This charge regulation model predicts that $R \propto \varepsilon_R^{-1}$, in which R is the radius of the POM-shells and ε_R the dielectric constant of the solvent in which they are dispersed, which has indeed been verified experimentally. In this model the free energy is assumed to depend on two fluctuating and dependent variables: its aggregation number, reflected in the radius R, and the effective charge Z. The free energy of a POM-shell F in the limit of $\kappa^{-1} \gg R$ can then be described by[5]

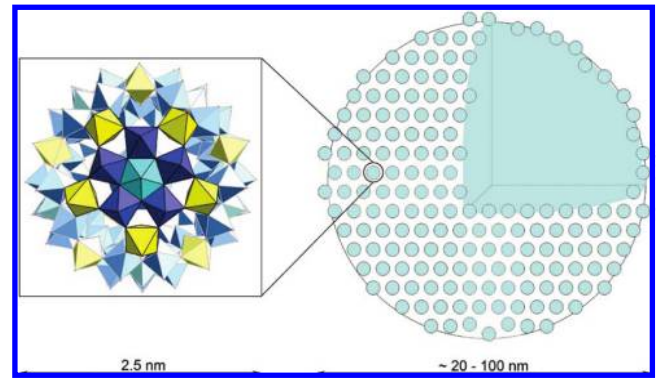

Figure 1. Schematic representation of a hollow spherical superstructure of polyoxometalates (POM-shells). Polyoxometalates (POMs) have been shown to spontaneously form POM-shells, which contain up to a 1000 of individual POMs and can grow up to several tens of nanometers in water. In this example the POM-shell contains the 2.5 nm large POM abbreviated as $\{Mo_{72}Fe_{30}\}$. Sizes of the POM-shell indicated refer to the size range in aqueous solutions.

* Corresponding author. E-mail: w.k.kegel@uu.nl.

10.1021/jp907631a CCC: $40.75
Published on Web 10/16/2009

$$\frac{F}{kT} = 4\pi\gamma_0 R^2 - 12u + \frac{\lambda_B Z^2}{2R(1+\kappa R)} - \psi Z \qquad (\kappa^{-1} \gg R) \quad (1)$$

in which γ_0 denotes the surface tension, u is the cohesive bond energy between two POMs in the POM-shell, ψ is the zeta potential, $\lambda_B = (e^2)/(4\pi\varepsilon_0\varepsilon_R kT)$ is the Bjerrum length, and $\kappa = (8\pi\lambda_B\rho_s)^{1/2}$ the inverse Debye screening length, with k being the Boltzmann's constant, T is the absolute temperature, e is the unit charge, ε_0 is the permittivity of vacuum, ε_R is the relative permittivity of the medium, and ρ_s is the number density of the 1:1 electrolyte.

The formation of the POM-shells occurs under conditions of low ionic strength. The validity of eq 1 requires that counterions inside the shell can be neglected, hence, $R \ll \kappa^{-1}$. In this case, the shell can be approximated by a charged sphere that is reflected in the third term in eq 1. This term arises from the screened-Coulomb interactions on a uniformly charged sphere in a background electrolyte characterized by a Debye screening length κ^{-1}, within the Debye−Hückel approximation.[8]

At higher salt concentrations, however, counterions inside the shell can no longer be neglected. In that case, the electrostatic energy can not be described by the third term in eq 1. As a limiting case, the system can than be described by a charged shell with a continuous distribution of point charges.[9] The third term should in that case be replaced by

$$\frac{\lambda_B Z^2}{2\kappa R^2}(1 - e^{-2\kappa R}) \qquad (\kappa^{-1} \ll R) \quad (2)$$

in the limit of $\kappa^{-1} \ll R$. This leads to a different behavior of the free energy with respect to the size of the system. It can be verified that, replacing the third term in eq 1 by eq 2, the free energy per unit area of the shell monotonically decreases with R. In this limit the shells will no longer be stable and will grow to have an infinite size. In the other limit, where the third term in eq 1 applies and in which $\kappa^{-1} \gg R$, the free energy per unit area of the shell has a minimum corresponding to the optimal radius of the system.

One can also understand this result from another point of view. As soon as κ^{-1} becomes smaller than the radius of the shell, the interactions between the POMs in the shell become of shorter range than the size of the system. In this case the electrostatic interactions between the POMs are not able to prevent the system from growing and the shells can grow to have an infinite radius. In practice this means that no finite-sized shells can be stable above a certain salt concentration, leading to a limit in its structural stability.

This structural stability limit was determined experimentally for POM-shells of a C_{60}-like, hollow, spherically shaped, Keplerate-type POM of 2.5 nm in diameter. It has the following composition in its crystalline state[10]

$$Mo^{VI}_{72}Fe^{III}_{30}O_{252}(CH_3OO)_{12}\{Mo_2O_7(H_2O)\}_2 \times \{H_2Mo_2O_8(H_2O)\}(H_2O)_{91}\bullet ca.150(H_2O)$$

and was prepared according to established procedures.[11] It will further be referred to as $\{Mo_{72}Fe_{30}\}$ (Figure 2). When dissolved into aqueous solution, $\{Mo_{72}Fe_{30}\}$ acts as a weak acid. Water molecules coordinated to the iron atoms in the structure can partially deprotonate resulting in a negative charge.[10]

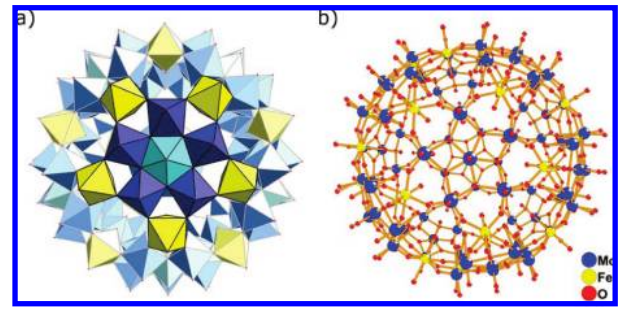

Figure 2. Schematic representations of the polyoxometalate (POM) $\{Mo_{72}Fe_{30}\}$. (a) Polyhedral representation. (b) Molecular representation. In polyhedral representation the metal atoms are located in the center and the oxygen atoms on the corners of the polyhedra. The inorganic macro ion is spherically symmetric, has a diameter of 2.5 nm, and consists of 12 5-fold symmetrical units (blue and turquoise) linked by 30 iron groups (yellow).

The point at which POM-shells of $\{Mo_{72}Fe_{30}\}$ are no longer stable was determined by preparing a dilution series with different concentrations of NaCl in Milli-Q water. The added NaCl concentrations ranged from 0 to 50.0 mM. Subsequently, weighed amounts of solid $\{Mo_{72}Fe_{30}\}$ were dissolved in the different salt containing aqueous solutions so that each sample contained 0.1 mg/mL of the POM. The formation of the POM-shells in solutions of $\{Mo_{72}Fe_{30}\}$ is extremely slow, particularly at room temperature. The samples were therefore heated to 55 °C for 15 weeks.

After this period, visual observation revealed that no large structures were present in samples with 5.00 mM and higher salt concentrations. A hand-held laser (Helium−Neon, Hughes, model 435LF4) directed through the samples showed strong scattering in the samples with no added salt and with a concentration of 1.00 mM of NaCl (see Figure 3). All samples containing a higher salt concentration did not show scattering. At the same time a yellow precipitate was observed in salt concentrations higher than 1.00 mM. Where the solutions of 0 and 1.00 mM added NaCl had a yellow color due to the dissolution of $\{Mo_{72}Fe_{30}\}$, the solutions containing higher salt concentration were colorless. These observations were confirmed by UV−visible spectroscopy experiments perfomed on a Cary 1E UV−visible spectrophotometer at room temperature in quartz cuvets. $\{Mo_{72}Fe_{30}\}$ has a characteristic absorption peak at 333 nm.[11] Therefore, the transmittance of the aqueous solutions at this wavelength was measured as a function of the concentration of added salt, the results of which are shown in Figure 3. For the samples containing 5.00 mM of added NaCl and higher, the samples transmitted on average 75% of the incomming light. If the loss of light in these samples is the result of absorption of single molecules of $\{Mo_{72}Fe_{30}\}$ only, the concentration of single POMs can be calculated from the extinction coefficient. The measured absorption in that case would correspond to $\{Mo_{72}Fe_{30}\}$ concentrations ranging from 0.006 to 0.01 mg/mL. A decrease in transmittance can be the result of an increase of absorption as well as loss of light by scattering of particles in solution. The samples containing 0 and 1.00 mM of added salt both had a significantly lower transmittance than the other samples. This effect can be explained both by the presence of a higher concentration of single POMs and thus a higher absoption, as well as from the loss of light by scattering of the POM-shells. The difference in transmittance between 0 and 1.00 mM of added NaCl can be explained largely due to a higher

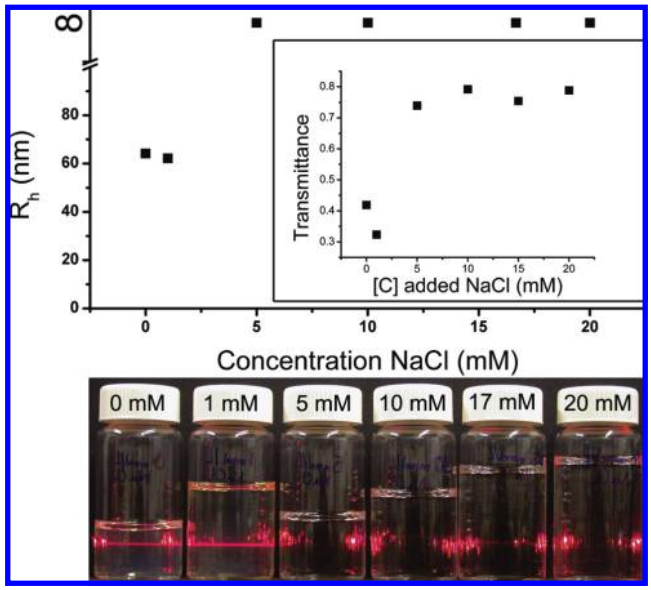

Figure 3. Effect of salt addition on the stability of POM-shells of $\{Mo_{72}Fe_{30}\}$. The hydrodynamic radii of the POM-shells measured with dynamic light scattering for the different salt contaning solutions are shown with underneath the graph a photograph of the different salt containing aqueous solutions of 0.1 mg/mL $\{Mo_{72}Fe_{30}\}$. A red hand-held laser was directed from right to left through the glass screw cap vials. No significant scattering of the beam can be distinguished for samples with 5.00 mM NaCl and higher. Inlay: Transmittance at 333 nm of aqueous solutions of $\{Mo_{72}Fe_{30}\}$ containing different concentrations of added salt. The transmittance of light of 333 nm is significantly lower for the samples containing 0 and 1.00 mM of added NaCl then for samples containing higher amounts of added salt.

amount of single free POMs in the sample leading to a higher contribution of the absorption.

Dynamic light scattering measurements of the samples containing 0 and 1.00 mM of added NaCl were done on an in house setup with an argon-ion laser (Spectra Physics) operating at a wavelength of 514.5 nm and a temperature of 298 K. The autocorrelation functions were recorded with a multiple tau digital correlator (ALV, type 6010/160). The samples were cooled to room temperature and filtered with a Whatman, Schleicher, and Schuell FP30/0,45 CA-S, cellulose acetate filter with pores of 450 nm mounted on a syringe. Measurements were performed in glass Danliker cuvets which were rinsed with freshly distilled acetone. Hydrodynamic radii where recorded at angles in between 35 and 120°. These measurements revealed objects with an average hydrodynamic radius of 64.17 ± 1.15 nm and 62.16 ± 0.57 nm for 0 and 1.00 mM of added NaCl respectively, which is in agreement with sizes measured previously for these systems.[5]

Althought the formation of POM-shells in aqueous solutions of $\{Mo_{72}Fe_{30}\}$ is well established (see for instance refs 12−14), the formation of shells in these type of solutions was verified with help of analytical ultracentrifugation. Sedimentation velocity experiments were performed on a sample containing no added salt with a concentration of 0.5 mg/mL of $\{Mo_{72}Fe_{30}\}$. Dynamic light scattering revealed objects with a hydrodynamic radius of $R_h = 57.70 \pm 5.00$ nm in this sample. Although the concentration of POMs in this particular sample is higher than for the samples used in the salt series, the size of the species in solution is in good agreement with what is found in both the sample with 1.00 mM added NaCl and no added salt of 0.1 mg/mL $\{Mo_{72}Fe_{30}\}$.

Sedimentation velocity experiments were performed after 2 weeks of heating at 55 °C on a Beckman Coultier Optima XL-A analytical ultracentrifuge. The sample was centrifuged at a speed of 6600 rpm at a temperature of 293 K, while the sedimentation profiles were recorded at a wavelength of 405 nm with help of absorbance optics. A sedimentation coefficient distribution was deduced by means of a Van Holde-Weichet[15] analysis, as presented in the program Ultrascan,[16] after subtraction of the time invariant noise obtained from a two-dimensional spectrum analysis.

The weight average sedimentation coefficient of the species in solution was determined to be $(6.00 \pm 2.15) \times 10^{-11}$ s. Together with the measured R_h of 57.70 nm it is clear that structures in solution are not solid, in which case the sedimentation coefficient for particles with a radius of 57.70 nm would have been 182.8×10^{-11} s. If one were to assume that the species in solution in the sample consist of POM-shells with a shell thickness for which the mass is then proportional to the square of the radius, this thickness can be calculated by means of

$$s = \frac{m_b}{f} \equiv \frac{2}{3}\frac{R_h \delta_l (\rho_l - \rho_s)}{\eta_s} \tag{3}$$

with $m_b \equiv 4\pi R_h^2 \delta_l (\rho_l - \rho_s)$, f is the friction coefficient which for a sphere is equal to $6\pi\eta_s R_h$, δ_l is the thickness of the layer, ρ_l is the density of a layer, ρ_s is the density of the solvent, and η_s is the solvent viscosity. The weight average sedimentation coefficient is consistent with a shell of about 1 to 2 POM diameters in thickness if hexagonal packing of the POMs in the layers is assumed.

As for the salt containing aqueous solutions of $\{Mo_{72}Fe_{30}\}$, the experiments presented here indicate that the structural stability limit of POM-shells of $\{Mo_{72}Fe_{30}\}$ lies between 1.00 and 5.00 mM NaCl. The salt concentration of 1.00 mM corresponds to $\kappa^{-1} = 10$ nm, which is the same order of magnitude as the measured 60 nm radius of the POM-shells. This result is in line with the predictions made on the basis of the charge regulation model. Previously reported stability limits of $\{Mo_{72}Fe_{30}\}$ in aqueous NaCl solutions are orders of magnitude larger than the stability limit found here (∼51 mM in ref 6 and 85 mM in ref 7). At these high salt concentrations, however, POM-shells display a colloidal instability as is evident, among other things, by the Schultz-Hardy rule.[8] Due to screening of the Coulomb interactions, the POM-shells themselves aggregate and subsequently precipitate out of solution. The structure of the shells, however, remains intact under those conditions. Colloidal instabilities are already apparent after approximately a day. Only close to the critical salt concentration the time scale lengthens to 30 days at most. This time scale is relatively short compared to the time scales connected to the stability limit found here. The theory summarized above describes an instability due to a structural change in the POM-shells. The activation barriers for structural changes in this system are high, as is evident from the slow formation process of the POM-shells.[14] Considering these slow dynamics, the structural stability limit requires significantly more time to become evident.

In conclusion, we show here that systems of POM-shells can display two types of instabilities: colloidal instability as well as a new structural instability. Between a NaCl concentration of 1.00 and 5.00 mM in water POM-shells of $\{Mo_{72}Fe_{30}\}$ become unstable due to this structural instability. Above a NaCl concentration of ∼51 mM the POM-shells will become unstable due to a colloidal instability. POM-shells formed by different

kinds of POMs are governed by the same free energy.[5] It is therefore expected that these will also display a structural stability limit, pointing to a general behavior for this type of shell-forming systems.[2−4] The combination of both a structural and a colloidal stability limit in shell-like systems occurring at different time scales offers interesting possibilities in for instances the controlled capture and release of materials. The issue of control over the (long) time scale of the structural instability, however, offers an interesting challenge.

References and Notes

(1) Müller, A.; Diemann, A.; Kuhlmann, C.; Eimer, W.; Serain, C.; Tak, T.; Knöchel, A.; Pranzas, P. *Chem. Commun.* **2001**, *2001*, 1928.

(2) Liu, T.; Diemann, E.; Li, H.; Dress, A.; Müller, A. *Nature* **2003**, *426*, 59–62.

(3) Liu, G.; Liu, T.; Mal, S.; Kortz, U. *J. Am. Chem. Soc.* **2006**, *128*, 10103–10110.

(4) Li, D.; Zhang, J.; Landskron, K.; Liu, T. *J. Am. Chem. Soc.* **2008**, *130*, 4226–4227.

(5) Verhoeff, A. A.; Kistler, M. L.; Bhat, A.; Pigga, J.; Groenewold, J.; Klokkenburg, M.; Veen, S. J.; Roy, S.; Liu, T.; Kegel, W. K. *Phys. Rev. Lett.* **2007**, *99*, 066104.

(6) Liu, G.; Cai, Y.; Liu, T. *J. Am. Chem. Soc.* **2004**, *126*, 16690–16691.

(7) Liu, G.; Cons, M.; Liu, T. *J. Mol. Liq.* **2005**, *118*, 27–29.

(8) Hunter, R. J. *Foundations of Colloid Science*, 2nd ed.; Oxford University Press: New York; 2001.

(9) Lyulin, S. V.; Evers, L. J.; Van der Schoot, P.; Darinskii, A. A.; Lyulin, A. V.; Michels, M. A. J. *Macromolecules* **2004**, *37*, 3049–3063.

(10) Liu, T.; Imber, B.; Diemann, E.; Liu, G.; Cokleski, K.; Li, H.; Chen, Z.; Müller, A. *J. Am. Chem. Soc.* **2006**, *128*, 15914–15920.

(11) Müller, A.; Sarkar, S.; Shah, S.; Bögge, H.; Schmidtmann, M.; Sarkar, S.; Kögerler, P.; Hauptfleisch, B.; Trautwein, A.; Schünemann, V. *Angew. Chem., Int. Ed.* **1999**, *38*, 3238–3241.

(12) Liu, G.; Liu, T. *J. Am. Chem. Soc.* **2005**, *127*, 6942–6943.

(13) Liu, G.; Liu, T. *Langmuir* **2005**, *21*, 2713–2720.

(14) Liu, T. *J. Am. Chem. Soc.* **2003**, *125*, 312–313.

(15) Demeler, B.; van Holde, K. E. *Anal. Biochem.* **2004**, *335*, 279–288.

(16) Demeler, B. *Ultrascan 9.9; A Comprehensive Data Analysis Software Package for Analytical Ultracentrifugation Experiments*; The University of Texas Health Science Center at San Antonio, Department of Biochemistry: San Antonio, Texas.

JP907631A